Inorganic Chemistry

Article

pubs.acs.org/IC

Synthesis, Characterization, and Antitumor Activity of Water-Soluble (Arene)ruthenium(II) Derivatives of 1,3-Dimethyl-4-acylpyrazolon-5-ato Ligands. First Example of Ru(arene)(ligand) Antitumor Species Involving Simultaneous Ru−N7(guanine) Bonding and Ligand Intercalation to DNA

Francesco Caruso,*[,†] Elena Monti,[‡] Julian Matthews,[†] Miriam Rossi,[†] Marzia Bruna Gariboldi,[‡] Claudio Pettinari,[§] Riccardo Pettinari,[⊥] and Fabio Marchetti*[,⊥]

[†]Department of Chemistry, Vassar College, Poughkeepsie, New York 12604-0484, United States

[‡]Department of Theoretical and Applied Sciences, Division of Biomedical Sciences, University of Insubria, Via A. da Giussano 10, 21052 Busto Arsizio, Varese, Italy

[§]School of Science and Technology, Chemistry Section, University of Camerino, Via S. Agostino 1, 62032 Camerino Italy

[⊥]School of Pharmacy, Chemistry Section, University of Camerino, Via S. Agostino 1, 62032 Camerino Italy

Supporting Information

ABSTRACT: We report on the synthesis of novel water-soluble [(arene)Ru^{II}(Q)Cl] and [(arene)Ru^{II}(Q)(X)]BF_4 compounds (arene = *p*-cymene, benzene, hexamethylbenzene; HQ = 1,3-dimethyl-4-R-(C═O)-5-pyrazolone, HQ^{Me}, R = methyl, HQ^{Ph}, R = phenyl, HQ^{Naph}, R = naphthyl; X = H_2O, 9-ethylguanine), and their *in vitro* antitumor activity toward the cell lines MCF7 (HTB-22, human breast adenocarcinoma), HCT116 (CCL-247, human colorectal carcinoma), A2780 (human ovarian carcinoma), A549 (CCL-185, human lung carcinoma), and U87 MG (HTB-1, human glioblastoma). The X-ray crystal structures of two complexes were determined. One of them, {chlorido-(*p*-cymene)-[(1,3-dimethyl-4-(1-naphthoyl)-pyrazolon-5-ato]ruthenium(II)}, was also studied with density functional theory methods and was selected for docking on a DNA octamer showing intercalation between DNA bases by the naphthyl moiety and for Ru−N7(guanine) bonding.

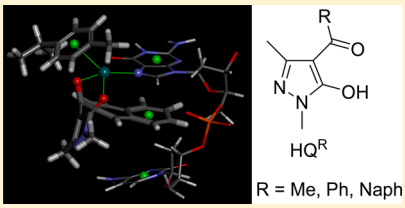

1. INTRODUCTION

The design of antitumor ruthenium complexes has been of increasing interest after two Ru^{III} species, imidazolium-(imidazole)(dimethylsulfoxide)tetrachlororuthenate(III) (NAMI-A) and indazolium *trans*-[tetrachlorobis(1H-indazole)-ruthenate(III)] (KP1019) entered clinical trials.[1,2] Some features of these compounds suggested potential metal reduction to Ru^{II}, and compounds of the type $Ru^{II}(\eta^6$-arene) explored by Sadler also were found to be active.[3] Compounds incorporating the 1,3,5-triaza-7-phosphaadamantane (PTA) ligand, for example, [Ru(η^6-*p*-cymene)(PTA)Cl_2] (RAPTA-C), show activity against metastases, and a pH-dependent interaction with DNA was suggested as a key component.[4] Recent studies on arene−Ru^{II}−chloroquine complexes have demonstrated their interaction with DNA and their ability to induce apoptosis on human lymphoid cell lines.[5] Studies involving natural ligands included in the Ru coordination sphere have been undertaken as well.[6,7]

Compounds of the type [(η^6-arene)Ru(X)(YZ)] (where YZ is a bidentate chelating ligand and X a good leaving group, e.g. Cl^-) exhibit both *in vitro* and *in vivo* anticancer activity, in some cases even comparable to that of cisplatin.[8] The aqueous reactivity of [(η^6-arene)Ru(X)(YZ)] complexes is highly dependent on the nature of X, YZ, and the arene.[9,10] [(η^6-arene)Ru(ethylenediamine)Cl]$^+$ complexes exhibit anticancer activity both *in vitro* and *in vivo*, including cisplatin-resistant cancer cells.[11] The hydrolysis of the metal-chloride bond appears to be important for activation, giving aqua adducts[9] [(η^6-arene)Ru(ethylenediamine)(H_2O)]$^{2+}$ that can bind to DNA (or proteins), forming monofunctional adducts. Studies in aqueous solution have shown that [(η^6-biphenyl)Ru-(ethylenediamine)]$^{2+}$ binds specifically to guanine when in competition with adenine, cytosine, and thymine nucleotides,[11] and similarly to plasmid DNA.[12] Moreover, guanine binds strongly through N7 with additional formation of a strong H-bond between C6O(guanine) and NH(ethylenediamine).[13] The possibility of arene intercalation between the DNA bases has also been recognized.[13,14] Replacement of neutral ethylenediamine by anionic *β*-diketonates such as acetylacetonato (acac) showed that the chelating ligand increases the rate and extent of hydrolysis as well as raising the pK_a of the aqua complex.[15]

Received: December 30, 2013
Published: March 11, 2014

   dx.doi.org/10.1021/ic403170y | *Inorg. Chem.* 2014, 53, 3668−3677

We recently reported the synthesis of (arene)Ru^{II} curcumin derivatives displaying antitumor activity,[16] in which not only the metal fragment but also the chelating ligand is known to possess biological activity. The same approach guided us to synthesize similar (arene)Ru^{II} systems[17] containing a variant of classic β-diketonates that are well-known molecules with biological properties,[18] namely, the acylpyrazolonate ligands (Scheme 1),[19] where a pyrazole ring is fused to the O,O′-

Scheme 1. 4-Acyl-5-pyrazolone Ligand, Keto-Enol Form, Used in This Work (Q^{Me}, Q^{Ph}, and Q^{Naph})

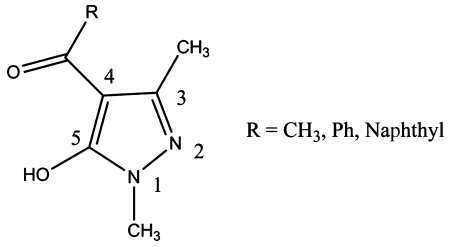

chelating moiety. Here we extend our studies to the design, synthesis, and characterization of novel (arene)Ru^{II} acylpyrazolonates, which are more soluble in water than the curcumin compounds, and test their antitumor activity on five tumor cell lines *in vitro*. We also describe successful docking features of one derivative onto a guanosine-containing DNA fragment.

EXPERIMENTAL SECTION

Chemicals and Reagents. All reactants were purchased from Alfa (Karlsruhe) and Aldrich (Milwaukee) and used as received. The samples for microanalyses were dried in vacuo to constant weight (20 °C, ca. 0.1 Torr). Elemental analyses (C, H, N, S) were performed in house with Fisons Instruments 1108 CHNS-O Elemental Analyzer. IR spectra were recorded from 4000 to 600 cm^{-1} with a Perkin-Elmer Spectrum 100 FT-IR instrument and from 600 to 200 cm^{-1} with a Perkin-Elmer System 2000 FT-IR instrument. ^1H and ^{13}C NMR spectra were recorded on a 400 Mercury Plus Varian spectrometer operating at room temperature (400 MHz for ^1H and 100 MHz for ^{13}C). Melting points were taken on an IA 8100 Electrothermal Instrument. The electrical conductance of the acetonitrile and water solutions was measured with a Crison CDTM 522 conductimeter at room temperature. Positive and negative electrospray mass spectra were obtained with a Series 1100 MSI detector HP spectrometer. Solutions (3 mg/mL) were used for electrospray ionization mass spectrometry (ESI-MS), and data, mass, and intensities were compared to those calculated using IsoPro Isotopic Abundance Simulator, version 2.1.16.

Synthesis of Acylpirazolone Ligands: HQ^{Naph}. 1,3-Dimethyl-4-(1-naphthoyl)-5-pyrazolone has been synthesized following a related procedure previously reported.[19] It is soluble in all common organic solvents, such as alcohols, acetone, acetonitrile, dimethyl sulfoxide (DMSO), and halogenated organic solvents. Yield 92%. Mp 177−180 °C. Anal. Calcd. for $C_{16}H_{14}N_2O_2$: C, 72.17; H, 5.30; N, 10.52%. Found: C, 71.84; H, 5.40, N, 10.34%. IR (nujol, cm^{-1}): 3370br ν(O−H···O), 1685m δ(O−H···O), 1614vs ν(C═O), 1588s ν(C═N + C═C). ^1H NMR ($CDCl_3$, 298 K, δ): 2.05s (3H, C3−CH_3), 3.68s (3H, N1−CH_3), 5.30br (1H, O−*H*), 7.60m, 7.68dd, 7.92m, 8.11dd, 8.70d (7H, $CH_{aromatic}$). $^{13}C\{^1H\}$ ($CDCl_3$, δ): 15.8 (C3−CH_3), 32.6 (N1−CH_3), 103.5 (*C*4), 124.5, 126.9, 127.1, 128.0, 128.1, 128.4, 128.6, 128.7, 129.0, 129.7 ($C_{aromatic}$), 147.2 (*C*3), 160.8, 170.1 (*C*5), 193.0 (CO). The other HQ ligands, namely, HQ^{Me} (1,3-dimethyl-4-acetyl-5-pyrazolone) and HQ^{Ph} (1,3-dimethyl-4-benzoyl-5-pyrazolone), were synthesized as previously reported.[19]

Synthesis of Metal Complexes 1−9. *(1), [Chlorido(p-cymene)-(1,3-dimethyl-4-acetyl-5-pyrazolonato)ruthenium(II)], [Ru(η^6-p-cymene)(Q^{Me})Cl].* HQ^{Me} (0.154 g, 1 mmol) and NaOMe (0.054 g, 1 mmol) were dissolved in methanol (20 mL) and stirred for 30 min at room temperature; then, $[Ru(\eta^6\text{-}p\text{-cymene})Cl_2]_2$ (0.306 g, 0.5 mmol) was added to the red solution, which immediately changed to orange. After 4 h of stirring at room temperature, the clear orange solution was evaporated to dryness, and the residue was dissolved in dichloromethane (10 mL), from which a precipitate slowly formed, which was filtered off and dried under reduced pressure. The powder was identified as derivative **1**. Recrystallization in methanol at +4 °C slowly yielded orange-red crystals. The compound is soluble in water, alcohols, acetone, acetonitrile, DMSO, and halogenated organic solvents. Yield 66%. Mp 161−163 °C. Anal. Calcd. for $C_{17}H_{23}ClN_2O_2Ru$: C, 48.17; H, 5.47; N, 6.61%. Found: C, 47.88; H, 5.62, N, 6.36%. Λ_m (acetonitrile, 298K, 10^{-3} mol/L) 11.7 Ω^{-1} cm^2 mol^{-1}. Λ_m (water, 298K, 10^{-3} mol/L) 114.9 Ω^{-1} cm^2 mol^{-1}. IR (nujol, cm^{-1}): 1590vs ν(C═O), 1522m ν(C═N + C═C), 440s, 369m ν(Ru−O), 279s ν(Ru−Cl). ^1H NMR ($CDCl_3$, 298 K, δ): 1.27d, 1.34d (6H, J = 6.6 Hz, $CH_3-C_6H_4-CH(CH_3)_2$), 2.22s (3H, C(═O)CH_3, Q^{Me}), 2.27s (3H, $CH_3-C_6H_4-CH(CH_3)_2$), 2.37s (3H, C3−CH_3, Q^{Me}), 2.95sp ((septet), 1H, $CH_3-C_6H_4-CH(CH_3)_2$), 3.45s (3H, N1−CH_3, Q^{Me}), 5.25d, 5.52d (4H, AA′BB′ system, $CH_3-C_6H_4-CH(CH_3)_2$). ^1H NMR (D_2O, 298 K, δ): 0.99d, 1.08d (6H, J = 6.6 Hz, $CH_3-C_6H_4-CH(CH_3)_2$), 1.93s (3H, C(═O)CH_3, Q^{Me}), 2.05s (3H, $CH_3-C_6H_4-CH(CH_3)_2$), 2.16s (3H, C3−CH_3, Q^{Me}), 2.68sp ((septet), 1H, $CH_3-C_6H_4-CH(CH_3)_2$), 3.53s (3H, N1−CH_3, Q^{Me}), 5.58d, 5.74d (4H, AA′BB′ system, $CH_3-C_6H_4-CH(CH_3)_2$). $^{13}C\{^1H\}$ ($CDCl_3$, δ): 17.4 (C3−CH_3, Q^{Me}), 20.3 ($CH_3-C_6H_4-CH(CH_3)_2$), 21.8 ($CH_3-C_6H_4-CH(CH_3)_2$), 26.5 (C(═O)CH_3, Q^{Me}), 30.5 ($CH_3-C_6H_4-CH(CH_3)_2$), 32.6 (N1−CH_3, Q^{Me}), 78.8, 80.7, 81.4, 82.3, 96.8, 99.4 (C_6H_6, η^6-*p*-cymene), 105.1 (*C*4, Q^{Me}), 147.2 (*C*3, Q^{Me}), 161.9 (*C*5, Q^{Me}), 189.6 (*C*═O, Q^{Me}). $^{13}C\{^1H\}$ (D_2O, δ): 17.4 (C3−CH_3, Q^{Me}), 20.3 ($CH_3-C_6H_4-CH(CH_3)_2$), 21.8 ($CH_3-C_6H_4-CH(CH_3)_2$), 26.5 (C(═O)CH_3, Q^{Me}), 30.5 ($CH_3-C_6H_4-CH(CH_3)_2$), 32.6 (N1−CH_3, Q^{Me}), 80.4, 81.0, 81.3, 82.5, 98.6, 103.6 (C_6H_6), 104.4 (*C*4, Q^{Me}), 155.8 (*C*3, Q^{Me}), 161.2 (*C*5, Q^{Me}), 193.0 (C═O, Q^{Me}). ESI-MS (+) CH_3OH (*m*/*z*, relative intensity %): 388 [100] $[Ru(\eta^6\text{-}p\text{-cymene})(Q^{Me})]^+$.

(2), [Chlorido-(p-cymene)-(4-benzoyl-1,3-dimethyl-pyrazolon-5-ato)ruthenium(II)], [Ru(η^6-p-cymene)(Q^{Ph})Cl]. Compound **2** was prepared following a procedure similar to that reported for **1**, starting from $[Ru(\eta^6\text{-}p\text{-cymene})Cl_2]_2$ (0.306 g, 0.5 mmol), HQ^{Ph} (0.216 g, 1 mmol), and NaOMe (0.054 g, 1 mmol). The compound is soluble in water, alcohols, acetone, acetonitrile, DMSO, and halogenated organic solvents. Yield 68%. Mp 187−191 °C. Anal. Calcd. for $C_{22}H_{25}ClN_2O_2Ru$: C, 54.37; H, 5.19; N, 5.76%. Found: C, 54.02; H, 5.35, N, 5.45%. Λ_m (acetonitrile, 298K, 10^{-3} mol/L) 8.4 Ω^{-1} cm^2 mol^{-1}. Λ_m (water, 298K, 10^{-3} mol/L) 121.6 Ω^{-1} cm^2 mol^{-1}. IR (nujol, cm^{-1}): 1594vsν (C═O), 1572, 1522, 1501 ν(C═C, C═N), 443s, 427m, 367m ν(Ru−O), 281s ν(Ru−Cl). ^1H NMR ($CDCl_3$, 298 K, δ): 1.29d, 1.35d (6H, $CH_3-C_6H_4-CH(CH_3)_2$), 1.57s (3H, C3−CH_3, Q^{Ph}), 2.27s (3H, $CH_3-C_6H_4-CH(CH_3)_2$), 2.95sp ((septet), 1H, $CH_3-C_6H_4-CH(CH_3)_2$), 3.43s (3H, N1−CH_3, Q^{Ph}), 5.25d, 5.55d (4H, AA′BB′ system, $CH_3-C_6H_4-CH(CH_3)_2$), 7.42m (5H, C(═O)C_6H_5). ^1H NMR (D_2O, 298 K, δ): 1.09d, 1.12d, 1.21d, 1.24d (6H, $CH_3-C_6H_4-CH(CH_3)_2$), 1.86s, 2.06s (3H, $CH_3-C_6H_4-CH(CH_3)_2$), 1.95s, 2.14s (3H, C3−CH_3), 2.74m (1H, $CH_3-C_6H_4-CH(CH_3)_2$), 3.42s (3H, N1−CH_3), 5.50t, 5.59d, 5.74t, 5.84d (4H, AA′BB′ system, $CH_3-C_6H_4-CH(CH_3)_2$), 7.41m, 7.52m (5H, C(═O)C_6H_5). $^{13}C\{^1H\}$ ($CDCl_3$, δ): 16.2 (C3−CH_3), 18.1 ($CH_3-C_6H_4-CH(CH_3)_2$), 22.1, 22.3, 22.5 ($CH_3-C_6H_4-CH(CH_3)_2$), 30.8, 31.0 ($CH_3-C_6H_4-CH(CH_3)_2$), 32.1 (N1−CH_3), 78.7, 79.0, 80.7, 81.5, 82.4, 82.8, 96.9, 99.5 ($CH_3-C_6H_4-CH(CH_3)_2$), 127.9, 128.1, 130.4, 138.9 (C(═O)C_6H_5), 106.1 (*C*4), 147.7 (*C*3), 164.0 (*C*5), 187.8 (CO). ESI-MS (+) CH_3OH (*m*/*z*, relative intensity %): 450 [100] $[Ru(\eta^6\text{-}p\text{-cymene})(Q^{Ph})]^+$.

(3), {Chlorido-(p-cymene)-[(1,3-dimethyl-4-(1-naphthoyl)-pyrazolon-5-ato]ruthenium(II)}, [Ru(η^6-p-cymene)(Q^{Naph})Cl]. It was prepared following a procedure similar to that reported for **1**, starting from $[Ru(\eta^6\text{-}p\text{-cymene})Cl_2]_2$ (0.306 g, 0.5 mmol), HQ^{Naph} (0.266 g, 1 mmol), and NaOMe (0.054 g, 1 mmol). The compound is soluble in water, alcohols, acetone, acetonitrile, DMSO, and halogenated organic

dx.doi.org/10.1021/ic403170y | Inorg. Chem. 2014, 53, 3668−3677

solvents. Yield 77%. Mp 104−106 °C. Anal. Calcd. for $C_{26}H_{27}ClN_2O_2Ru$: C, 58.26; H, 5.08; N, 5.23%. Found: C, 57.97; H, 5.18, N, 5.14%. Λ_m (acetonitrile, 298K, 10^{-3} mol/L) 5.7 Ω^{-1} cm^2 mol^{-1}. Λ_m (water, 298K, 10^{-3} mol/L) 108.4 Ω^{-1} cm^2 mol^{-1}. IR (nujol, cm^{-1}): 1589vs ν(C═O), 479s, 456s, 363m ν(Ru−O), 280s ν(Ru−Cl). ^{1}H NMR ($CDCl_3$, 298 K, δ): 1.37d, 1.40d (6H, CH_3−C_6H_4−$CH(CH_3)_2$), 1.59s (3H, C3−CH_3, Q^{Naph}), 2.28s (3H, CH_3−C_6H_4−$CH(CH_3)_2$), 2.99sp ((septet), 1H, CH_3−C_6H_4−$CH(CH_3)_2$), 3.52s (3H, N1−CH_3, Q^{Naph}), 5.31d, 5.58d (4H, AA′BB′ system, CH_3−C_6H_4−$CH(CH_3)_2$), 7.57m, 7.90m (6H, C−H_{naph}, Q^{Naph}), 8.62d (1H, C8−H_{naph}, Q^{Naph}). ^{13}C{^{1}H} ($CDCl_3$, δ): 16.4 (C3−CH_3, Q^{Naph}), 18.1 (CH_3−C_6H_4−$CH(CH_3)_2$), 22.5 (CH_3−C_6H_4−$CH(CH_3)_2$), 31.10 (CH_3−C_6H_4−$CH(CH_3)_2$), 32.2 (N1−CH_3, Q^{Naph}), 78.8, 79.1, 82.5, 82.7, 96.9, 99.5 (C_6H_6, η^6-p-cymene), 105.8 ($C4$, Q^{Naph}), 125.1, 126.9, 127.5, 128.0, 128.2, 128.8, 129.8, 131.9, 132.5, 134.3 (C_{naph}, Q^{Naph}), 136.2 ($C5$, Q^{Naph}), 147.8 ($C3$, Q^{Naph}), 187.7 (C═O, Q^{Naph}). ESI-MS (+) CH_3OH (m/z, relative intensity %): 501 [100] [Ru(η^6-p-cymene)(Q^{Naph})]$^+$.

(4), [Chlorido-(η^6-benzene)-(1,3-dimethyl-4-acetyl-5-pyrazolonato)ruthenium(II)], [Ru(η^6-benzene)(Q^{Me})Cl]. It was prepared following a procedure similar to that reported for **1**, starting from [Ru(benzene)Cl_2]$_2$ (0.250 g, 0.5 mmol), HQ^{Me} (0.154 g, 1 mmol), and NaOMe (0.054 g, 1 mmol). The compound is soluble in water, alcohols, acetone, acetonitrile, DMSO, and slightly soluble in halogenated organic solvents. Yield 74%. Mp 196−200 °C dec. Anal. Calcd. for $C_{13}H_{15}ClN_2O_2Ru$: C, 42.45; H, 4.11; N, 7.62%. Found: C, 42.21; H, 4.25, N, 7.85%. Λ_m (acetonitrile, 298K, 10^{-3} mol/L) 7.3 Ω^{-1} cm^2 mol^{-1}. Λ_m (water, 298K, 10^{-3} mol/L) 109.7 Ω^{-1} cm^2 mol^{-1}. IR (nujol, cm^{-1}): 1587vs ν(C═O), 1528m ν(C═C, C═N), 435vs, 369vs ν(Ru−O), 277vs ν(Ru−Cl). ^{1}H NMR ($CDCl_3$, 298 K, δ): 2.23s (3H, C(═O)CH_3, Q^{Me}), 2.38s (3H, C3−CH_3, Q^{Me}), 3.47s (3H, N1−CH_3, Q^{Me}), 5.69s (6H, C_6H_6, η^6-benzene). ^{1}H NMR (D_2O, 298 K, δ): 2.11s, 2.20s (3H, C3−CH_3), 2.33s, 2.44s (3H, C(═O)−CH_3), 3.32s, 3.57s (3H, N1−CH_3), 5.78s, 5.91s (6H, C_6H_6, η^6-benzene). ESI-MS (+) CH_3OH (m/z, relative intensity %): 332 [100] [Ru(η^6-benzene)(Q^{Me})]$^+$.

(5), [Chlorido-hexamethylbenzene-(1,3-dimethyl-4-acetyl-5-pyrazolonato)ruthenium(II)] [Ru(η^6-hmb)(Q^{Me})Cl]. It was prepared following a procedure similar to that reported for **1**, starting from [Ru(η^6-hexamethylbenzene)Cl_2]$_2$ (0.334 g, 0.5 mmol), HQ^{Me}(0.154 g, 1 mmol), and NaOMe (0.054 g, 1 mmol). The compound is soluble in water, alcohols, acetone, acetonitrile, DMSO, and halogenated organic solvents. Yield 76%. Mp 268−269 °C dec. Anal. Calcd. for $C_{19}H_{27}ClN_2O_2Ru$: C, 50.49; H, 6.02; N, 6.20%. Found: C, 50.23; H, 5.93, N, 6.09%. Λ_m (acetonitrile, 298K, 10^{-3} mol/L) 14.0 Ω^{-1} cm^2 mol^{-1}. Λ_m (water, 298K, 10^{-3} mol/L) 129.1 Ω^{-1} cm^2 mol^{-1}. IR (nujol, cm^{-1}): 1592vs ν(C═O), 1526m ν(C═C, C═N), 458s, 431vs, 365s ν(Ru−O), 281vs ν(Ru−Cl). ^{1}H NMR ($CDCl_3$, 298 K, δ): 2.07s (3H, C3−CH_3, Q^{Me}), 2.21s (18H, CH_3, η^6-hexamethylbenzene), 2.38s (3H, C(═O)−CH_3, Q^{Me}), 3.45s (3H, N1−CH_3, Q^{Me}). ESI-MS (+) CH_3OH (m/z, relative intensity %): 416 [100] [Ru(η^6-hmb)(Q^{Me})]$^+$.

(6) [Chlorido-hexamethylbenzene-(4-benzoyl-1,3-dimethyl-pyrazolon-5-ato)ruthenium(II)], [Ru(η^6-hmb)(Q^{Ph})Cl]. It was prepared following a procedure similar to that reported for **1**, starting from [Ru(η^6-hexamethylbenzene)Cl_2]$_2$ (0.334 g, 0.5 mmol), HQ^{Ph} (0.216 g, 1 mmol), and NaOMe (0.054 g, 1 mmol). The compound is soluble in water, alcohols, acetone, acetonitrile, DMSO, and halogenated organic solvents. Yield 81%. Mp 243−244 °C dec. Anal. Calcd. for $C_{24}H_{29}ClN_2O_2Ru$: C, 56.08; H, 5.69; N, 5.45%. Found: C, 55.38; H, 5.48, N, 5.29%. Λ_m (acetonitrile, 298K, 10^{-3} mol/L) 6.2 Ω^{-1} cm^2 mol^{-1}. Λ_m (water, 298K, 10^{-3} mol/L) 102.6 Ω^{-1} cm^2 mol^{-1}. IR (nujol, cm^{-1}): 1588vs ν(C═O), 1573m, 1520m ν(C═C, C═N), 460m, 449vs, 359m ν(Ru−O), 288vs ν(Ru−Cl). ^{1}H NMR ($CDCl_3$, 298 K, δ): 2.10s (3H, C3−CH_3, Q^{Ph}), 2.06s (18H, CH_3, η^6-hexamethylbenzene), 2.28s (3H, C(═O)−CH_3, Q^{Ph}), 3.15s (3H, N1−CH_3, Q^{Ph}), 7.39m (5H, N1−C_6H_5, Q^{Ph}). ESI-MS (+) CH_3OH (m/z, relative intensity %): 479 [100] [Ru(η^6-hmb)(Q^{Ph})]$^+$.

(7). [Aqua-(η^6-p-cymene)-(1,3-dimethyl-4-acetyl-5-pyrazolonato)ruthenium(II)] tetrafluoroborate, [Ru(η^6-p-cymene)-(Q^{Me})(H_2O)]BF_4. Derivative **1** (0.212 g, 0.5 mmol) was dissolved in acetonitrile/water (9:1) (10 mL); then, $AgBF_4$ (0.0.97 g, 0.5 mmol) was added to the solution, which was stirred for 2 h at room temperature. The solution was filtered to remove silver chloride; the solvent was removed in vacuo, and the residue was dried under reduced pressure. The powder was identified as derivative **7**, and it is soluble in acetone, acetonitrile, DMSO, and slightly soluble in water, alcohols, and halogenated organic solvents. Yield 85%. Mp 250 °C dec. Anal. Calcd. for $C_{17}H_{25}BF_4N_2O_3Ru$: C, 41.39; H, 5.11; N, 5.68%. Found: C, 41.74; H, 5.31, N, 5.36%. Λ_m (acetonitrile, 298K, 10^{-3} mol/L) 116.4 Ω^{-1} cm^2 mol^{-1}. IR (nujol, cm^{-1}): 3520br ν(H_2O), 1603vs ν(C═O), 1524m ν(C═C, C═N), 1047vs, 1030vs ν(BF_4), 986s, 453s br, 376m ν(Ru−O). ^{1}H NMR (CD_3CN, 298 K, δ): 1.34d, 1.37d (6H, J = 6.8 Hz, CH_3−C_6H_4−$CH(CH_3)_2$), 2.19s (3H, C(═O)CH_3, Q^{Me}), 2.25s (3H, CH_3−C_6H_4−$CH(CH_3)_2$), 2.44s (3H, C3−CH_3, Q^{Me}), 2.95sp ((septet), 1H, CH_3−C_6H_4−$CH(CH_3)_2$), 3.30br (2H, H_2O), 3.44s (3H, N1−CH_3, Q^{Me}), 5.52d, 5.83d (4H, AA′BB′ system, CH_3−C_6H_4−$CH(CH_3)_2$). ESI-MS (+) CH_3OH (m/z, relative intensity %): 388 [100] [Ru(η^6-p-cymene)(Q^{Me})]$^+$.

(8), {Aqua-(η^6-p-cymene)-[(1,3-dimethyl-4-(1-naphthoyl)-pyrazolon-5-ato]ruthenium(II)} tetrafluoroborate, [Ru(η^6-p-cymene)-(Q^{Naph})(H_2O)]BF_4. It was prepared following a procedure similar to that reported for **7**, starting from compound **3** (0.536 g, 1 mmol) and $AgBF_4$ (0.194 g, 1 mmol). The compound is soluble in water, alcohols, acetone, acetonitrile, DMSO, and partially soluble in halogenated organic solvents. Yield 70%. Mp 250 °C dec. Anal. Calcd. for $C_{26}H_{29}BF_4N_2O_3Ru$: C, 51.58; H, 4.83; N, 4.63%. Found: C, 51.30; H, 4.70, N, 4.48%. Λ_m (acetonitrile, 298K, 10^{-3} mol/L) 118.2 Ω^{-1} cm^2 mol^{-1}. IR (nujol, cm^{-1}): 3514sbr ν(H_2O), 1598vs ν(C═O), 1516m ν(C═C, C═N), 1003vsbr ν(BF_4). ^{1}H NMR (CD_3OD, 298 K, δ): 1.41d, 1.43d (6H, CH_3−C_6H_4−$CH(CH_3)_2$), 1.64s (3H, C3−CH_3, Q^{Naph}), 2.31s (3H, CH_3−C_6H_4−$CH(CH_3)_2$), 2.97sp ((septet), 1H, CH_3−C_6H_4−$CH(CH_3)_2$), 3.59s (3H, N1−CH_3, Q^{Naph}), 5.70d, 5.95d (4H, AA′BB′ system, CH_3−C_6H_4−$CH(CH_3)_2$), 7.61m, 8.02m (6H, C−H_{naph}, Q^{Naph}), 8.60d (1H, C−$H8_{naph}$, Q^{Naph}). ^{13}C{^{1}H} ($CDCl_3$, δ): 16.3 (C3−CH_3, Q^{Naph}), 18.0 (CH_3−C_6H_4−$CH(CH_3)_2$), 22.5 (CH_3−C_6H_4−$CH(CH_3)_2$), 32.4 (CH_3−C_6H_4−$CH(CH_3)_2$), 32.5 (N1−CH_3, Q^{Naph}), 79.6, 79.9, 80.1, 81.9, 98.9, 101.8 (C_6H_6, η^6-p-cymene), 105.8 ($C4$, Q^{Naph}), 125.6, 126.5, 127.9, 128.5, 128.9, 129.7, 130.5, 132.2, 133.9, 136.1 (C_{naph}, Q^{Naph}), 149.3 ($C5$, Q^{Naph}), 163.9 ($C3$, Q^{Naph}), 191.0 (C═O, Q^{Naph}). ESI-MS (+) CH_3OH (m/z, relative intensity %): 501 [100] [(p-cymene)Ru(Q^{Naph})]$^+$, 565 [60] [(p-cymene)Ru-(Q^{Naph})(CH_3OH)$_2$]$^+$.

(9), {(η^6-p-Cymene)-[(1,3-dimethyl-4-(1-naphthoyl)-pyrazolon-5-ato]-(9-ethylguanine)ruthenium(II)} tetrafluoroborate, [Ru(η^6-p-cymene)(Q^{Naph})(9-ethylguanine)]BF_4. Compound **8** (0.294 g, 0.5 mmol) was dissolved in a mixture of methanol−water (16:4 v/v), and 9-ethylguanine (0.089 g, 0.5 mmol) was added to the red solution. After 1 h of stirring at room temperature the solvent was removed in vacuo, and the residue was dried under reduced pressure. The resulting yellow powder was dried in air. The compound is soluble in acetone, acetonitrile, DMSO, and slightly soluble in water, alcohols, and halogenated organic solvents. Yield 85%. Mp 135 °C. Elem. Anal. Calcd. for $C_{33}H_{36}BF_4N_7O_3Ru$: C, 51.71; H, 4.73; N, 12.79%. Found: C, 51.60; H, 4.41, N, 12.52%. IR (nujol, cm^{-1}): 1579vs, 1569sh ν(C═O), 1542w, 1520w ν(C═C, C═N), 1051vs, 1000vs ν(BF_4). ^{1}H NMR (CD_3OD, 298 K, δ): 1.20t (3H, J = 7.2 Hz, CH_3−CH_2-9-ethylguanine), 1.29d, 1.31d (6H, 3H, J = 7.6 Hz, CH_3−C_6H_4−$CH(CH_3)_2$), 1.43s (3H, CH_3−C_6H_4−$CH(CH_3)_2$), 2.12s (3H, C3−CH_3, Q^{Naph}), 2.89sp (1H, J = 7.2 Hz, CH_3−C_6H_4−$CH(CH_3)_2$), 3.51s (3H, N1−CH_3, Q^{Naph}), 4.06q (2H, J = 7.2 Hz, CH_3−CH_2-9-ethylguanine), 5.67d, 5.92d (4H, AA′BB′ system, CH_3−C_6H_4−$CH(CH_3)_2$), 7.55m, 7.94m (6H, C−H_{naph}), 7.80s (1H, 9-ethylguanine), 8.60d (1H, C−$H8_{naph}$, Q^{Naph}). ^{13}C{^{1}H} (CD_3OD, δ): 15.8, 15.9 (C3−CH_3 and CH_3 of 9-ethylguanine), 18.2 (CH_3−C_6H_4−$CH(CH_3)_2$), 22.7, 22.8 (CH_3−C_6H_4−$CH(CH_3)_2$ and CH_2 of 9-ethylguanine), 32.3 (CH_3−C_6H_4−$CH(CH_3)_2$), 40.4 (N1−CH_3, Q^{Naph}), 81.6, 82.2, 84.9, 85.2, 100.2, 103.5 (CH_3−C_6H_4−$CH(CH_3)_2$), 105.8 ($C4$), 116.5 (9-ethylguanine), 125.8, 126.5, 127.9, 128.3, 128.9, 129.7, 132.1, 136.0, 136.8 (C_{naph}, Q^{Naph}), 141.1 (9-ethylguanine), 148.9 ($C3$, Q^{Naph}), 153.5, 156.1, 156.8 (9-ethylguanine), 164.5 ($C5$, Q^{Naph}),

dx.doi.org/10.1021/ic403170y | Inorg. Chem. 2014, 53, 3668−3677

Table 1. Crystal Data and Structure Refinement of Compounds 3 and 4

compound	3: [Ru(η^6-*p*-cymene)(Q^{Naph})Cl]	4: [Ru(η^6-benzene)(Q^{Me})Cl]
empirical formula	$C_{26}H_{27}ClN_2O_2Ru·H_2O$	$C_{13}H_{15}ClN_2O_2Ru$
formula weight	552.02	367.79
crystal system	monoclinic	monoclinic
space group	$P2_1/n$	$P2_1/n$
unit cell dimensions, Å	a = 9.6986(4)	a = 7.8172(16)
	b = 20.2270(8)	b = 17.886(4)
	c = 13.1742(5)	c = 9.5912(19)
unit cell dimensions, deg	β = 102.788(1)	β = 97.37(3)
volume (Å^3), crystal color	2520.32(17), red	1330.0(5), red
Z, T data collection (K)	4, 125	4, 125
density (calculated), Mg/m^3	1.455	1.837
absorption coefficient, mm^{-1}	0.577	1.378
crystal size, mm^3	0.31 × 0.29 × 0.19	0.33 × 0.31 × 0.09
theta range for data collection, deg	1.88 to 28.33	2.28 to 28.28
index ranges	$-12 \le h \le 12$, $-26 \le k \le 27$,	$-10 \le h \le 10$, $-23 \le k \le 23$,
	$-17 \le l \le 17$	$-12 \le l \le 12$
reflections collected	67009	16701
independent reflections	6263 [R(int) = 0.0278]	5711 [R(int) = 0.0209]
max. and min transmission	0.8695 and 0.7992	0.8860 and 0.6592
data/restraints/parameters	5541/0/386	3127/0/172
goodness-of-fit on F^2	1.081	1.298
final R indices [$I > 2\sigma(I)$]	$R1$ = 0.0441, $wR2$ = 0.1055	$R1$ = 0.0512, $wR2$ = 0.1492
R indices (all data)	$R1$ = 0.0522, $wR2$ = 0.1136	$R1$ = 0.0531, $wR2$ = 0.1501

190.1 (C═O, Q^{Naph}). ESI-MS (+) CH_3OH (m/z, relative intensity %): 501 [500] [(*p*-cymene)Ru(Q^{Naph})]$^+$, 680 [100] [(*p*-cymene)Ru-(Q^{Naph})(9-ethylguanine)]$^+$.

X-ray Diffraction Study. Crystals of **3** and **4** suitable for X-ray diffraction data collection were obtained by dissolving the samples in a mixture of 1:1 dichloromethane/methanol and on standing at room temperature for a week. Data were collected at 125 K using a Bruker SMART APEX II CCD X-ray diffractometer. Structure resolution and refinement were performed with SHELXTL;[20] details are included in Table 1. H atoms were calculated and constrained as riding on their bound atoms.

Theoretical Study. The theoretical study involved calculations using software programs from Accelrys.[21] Density functional theory (DFT) code DMol3 was applied to calculate energy, geometry, and frequencies implemented in Materials Studio 5.5 (PC platform).[22] We employed the double numerical polarized (DNP) basis set that includes all the occupied atomic orbitals plus a second set of valence atomic orbitals and polarized d-valence orbitals,[23] and correlation generalized gradient approximation (GGA) was applied in the manner suggested by Perdew-Burke-Ernzerhof (PBE);[24] these are the conditions for the highest-accuracy level available in DMol3. The spin unrestricted approach was exploited with all electrons considered explicitly. The real space cutoff of 5 Å was imposed for numerical integration of the Hamiltonian matrix elements. The self-consistent-field convergence criterion was set to the root-mean-square change in the electronic density to be less than 10^{-6} electron/Å^3. The convergence criteria applied during geometry optimization were 2.72 × 10^{-4} eV for energy and 0.054 eV/Å for force.

Cell Lines and in Vitro Culture Conditions. The cell lines MCF7 (HTB-22, human breast adenocarcinoma), HCT116 (CCL-247, human colorectal carcinoma), A549 (CCL-185, human lung carcinoma), and U-87 MG (HTB-1, human glioblastoma) were obtained from ATCC (American Type Culture Collection, Manassas, VA, USA); A2780 human ovarian carcinoma were obtained from ECACC (European Collection of Animal Cell Culture, Salisbury, U.K.). They were maintained under standard culture conditions (37 °C, 5% CO_2) in Dulbecco's Modified Eagle's medium (DMEM) (Euroclone, Milan, Italy), supplemented with 10% fetal calf serum (Euroclone, Milan, Italy), 1% glutamine, and 1% antibiotics mixture; for HCT116 and U-87 MG cells, 1% sodium pyruvate and 1% nonessential amino acids (both from Sigma-Aldrich, Milan, Italy) were also added to the culture medium. All experiments were performed within 10 passages from thawing.

Drugs. The four compounds under study were reconstituted in sterile DMSO at a concentration of 1 M; stock solutions were then diluted to the desired final concentrations with sterile complete medium immediately before each experiment. The final DMSO concentration never exceeded 0.2%, which was not toxic to the cells under the drug exposure conditions used in this study.

Growth Inhibition Assay. The 3-(4,5-dimethylthiazol-2-yl)-2,5-diphenyltetrazolium bromide (MTT) assay was performed on all the cell lines tested as described,[25] with minor modifications. Briefly, according to the growth profiles previously defined for each cell line, adequate numbers of cells were plated in each well of a 96-well plate in 0.1 mL of complete culture medium and allowed to attach for 24 h. Cells were exposed at 37 °C for 72 h to the four compounds at concentrations ranging between 5 and 750 μM, bringing the final volume to 0.2 mL/well. Each experiment included eight replications per concentration tested; control samples were run with 0.2% DMSO. At the end of the period of incubation, MTT (0.05 mL of a 2 mg/mL stock solution in phosphate-buffered saline (PBS)) was added to each well for 3 h at 37 °C. Cell supernatants were then carefully removed, the blue formazan crystals formed through MTT reduction by metabolically active cells were dissolved in 0.120 mL of DMSO, and the corresponding optical densities were measured at 570 nm, using a Universal Microplate Reader EL800 (Bio-TekWinooski, VT). IC_{50} values were estimated from the resulting concentration−response curves by nonlinear regression analysis, using GraphPad Prism software, v. 5.0 (GraphPad, San Diego, CA, USA). Differences between IC_{50} values were analyzed statistically by analysis of variance with Bonferroni post-test for multiple comparisons.

Docking Studies. These were performed with the molecular mechanics CDOCKER package, a grid-based molecular docking method that utilizes CHARMm[26] in Discovery Studio 3.5 from Accelrys.[21] We took advantage of our previous work,[16] where the keto−enol fragment in curcumin had few interactions with the DNA and was found to be energetically favored when pointing out of the helix. Our general strategy was to replace the Ru-curcuminato complex with [Ru(η^6-*p*-cymene)(Q^{Naph})Cl] (**3**) and minimize the system. Compound **3** was geometrically optimized from original X-ray

dx.doi.org/10.1021/ic403170y | Inorg. Chem. 2014, 53, 3668−3677

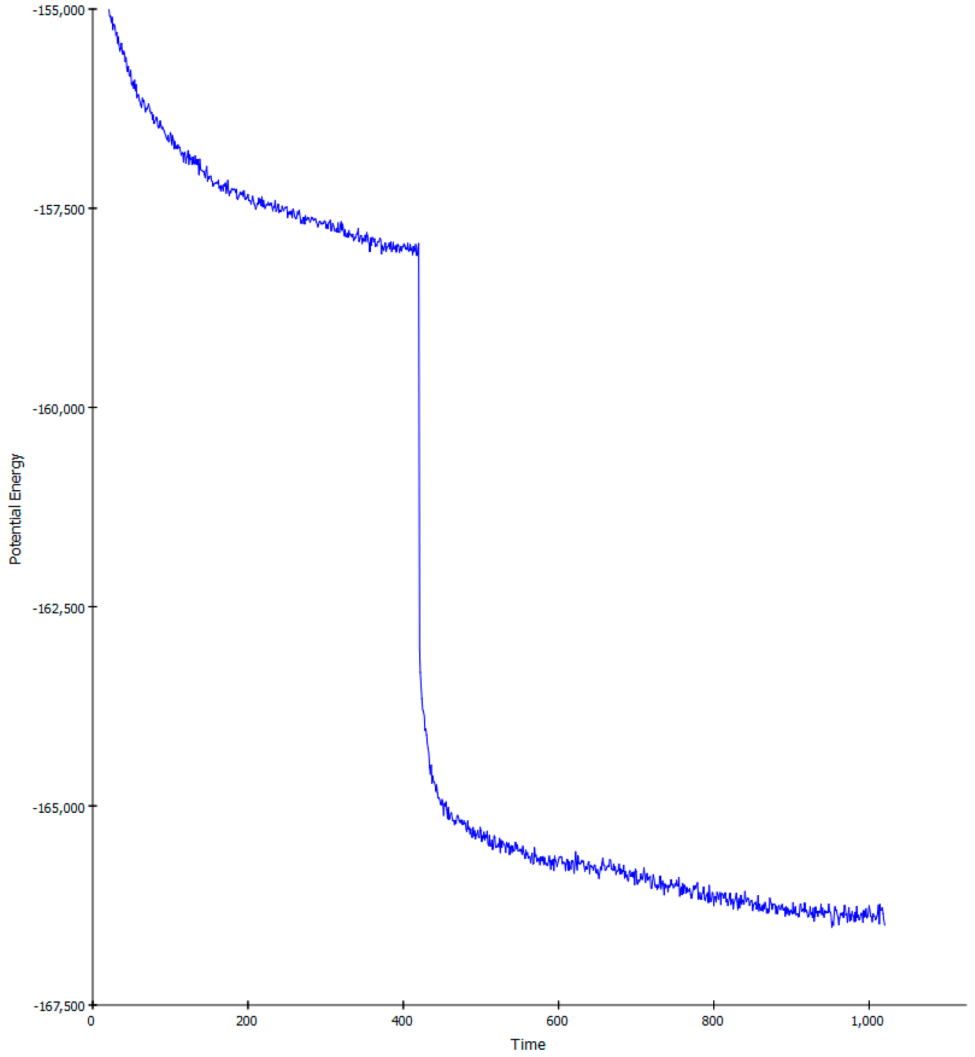

Figure 1. Development of potential energy (kcal/mol) vs conformation number for the dynamic cascade of the DNA model associated with compound **3**; conformation 952 has the minimum energy.

coordinates using the DFT program DMol3 (included in Materials Studio version 6.1 from Accelrys[21]) using the same setting earlier described for the (*p*-cymene)Ru(curcuminato)chloro complex.[16]

For the (*p*-cymene)Ru(curcuminato)chloro-DNA arrangement, the binding site was shown to be between the ruthenium and the guanine N7 helix. For the initial docking, complex **3** was graphically inserted into the double helix of a DNA octamer species deposited in the Protein Data Bank (www.Pdb.Org) (code 1N37).[27] 1N37 contains an intercalating antibody (respinomycin D), which was excised and replaced by **3** during the docking; one of the octamer's bases facing respinomycin D is guanine. We applied a solvation algorithm that provided 1868 H_2O molecules, 4 Cl^-, and 18 Na^+ ions. These, with the 14 negatively charged phosphate groups, make up a neutral system. We relocated the Cl^- anion of **3** into the solvent area since the expected reaction for the related Ru−Cl antitumor species is to cleave the Ru−Cl bond after entering the cell.[9]

After removing the Cl^- anion from **3**, we placed the corresponding cationic complex so that the Ru atom pointed to N7(guanine) along the same direction where the Cl was originally placed, for example, keeping the same bond angles for the coordination sphere. Then, we rotated the Ru cationic complex along the Ru−N7(guanine) axis so that the naphthyl moiety could be located in an area previously occupied by respinomycin D, that is, potentially establishing $\pi-\pi$ interactions. During this process we rotated the arene moiety along the Ru-arene centroid to avoid hindrance due to its isopropyl moiety.

Since the CHARMm forcefield does not include ruthenium bonding parameters, Ru was considered as an ion, similarly to our previous work.[16] Besides that, some constraints on bonds to optimize the minimization and docking were imposed: the last two base pairs from each end of the 1N37 were fixed, and various distances of the critical interactions between the cationic Ru complex and 1N37 were restrained: (1) Ru to N7 set at 2.1 Å; (2) distance restraint between Ru and the *p*-cymene centroid with an upper threshold of 1.9 Å and the lower of 1.8 Å; (3) all restraints included a force maximum and force constant maximum at 200 kcal/mol and a rigid body harmonic restraint at 10 kcal/mol.

In the Ru-curcuminato simulation[16] the water molecules surrounding the double helix were removed, and the counterions were maintained. For the present study we kept the solvent because the water molecules better mimic a biological environment. The dielectric constant was 4 as in the Ru-curcuminato simulation. Before our successful dynamics cascade we found out that typing/placing a forcefield on the molecules can modify the charge on specific atoms and had to reassign the partial charges on the complex, making O(carbonyl) {O(acyl) = Oa} as zero and O(anionic) {O(pyrazolonato = Op} as −1, respectively. In addition, as mentioned above, we assigned the Ru charge as +2, resulting in the remaining complex having a +1 charge. The objective was to minimize the distance between the ruthenium atom and N7(guanine) for ideal docking and to verify whether the potentially intercalated naphthyl moiety would stay in place. We first performed a 10 pose minimization as a

dx.doi.org/10.1021/ic403170y | *Inorg. Chem.* 2014, 53, 3668−3677

Scheme 2. Proligands HQ^R and Compounds 1−9

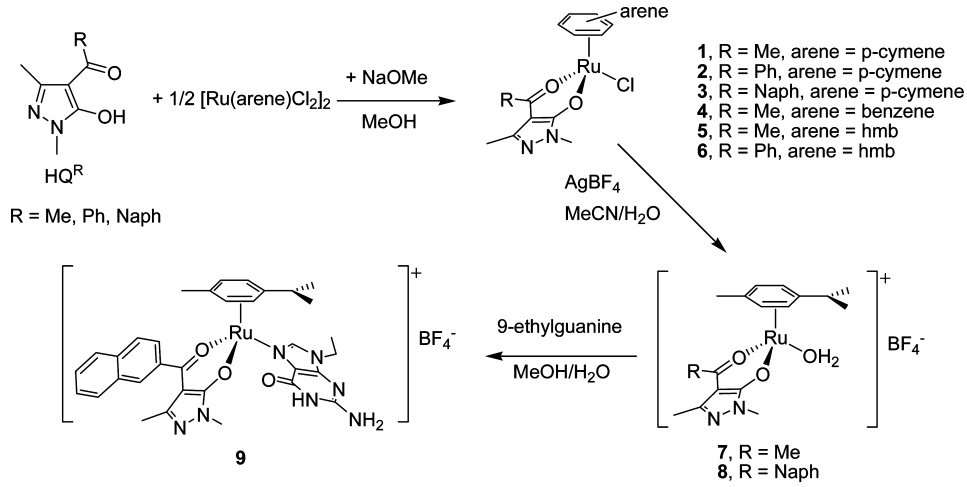

precautionary step for any obvious errors that may develop when performing a minimization (as the dynamics cascade produces hundreds of poses). The 10 poses were not very different from one another; however, the distance between Ru and N7 lengthened. Taking "bump" formation and chemically stable environments into consideration, the cationic Ru complex was manually docked to fit our aforementioned target criteria.

Subsequently, we performed the standard dynamics cascade. In the initial simulation the Ru−N bond increased to about 2.7 Å, which is consistent with the results obtained with Ru-curcuminato,[16] and so we increased the force maximum and force constant maximum to 1000 kcal/mol so as to afford a more realistic Ru−N bond distance. We also changed production to be 200 000 with save results frequency at 1000, 10 000 steps for heating and equilibration with save results frequency at 500. In summary, the standard dynamics cascade for 200 000 steps at a save results frequency at 100, results in 1000 conformations. Conformation 952 (−166 523 kcal/mol) showed the minimum potential energy, see Figure 1, and was much lower than conformation 1(−155 010 kcal/mol). The greatest decrease of energy was found after conformation 420, where the structure appears to find a region of the conformational space with more favorable electrostatic interactions.

RESULTS AND DISCUSSION

By interaction in methanol of proligands HQ^R and $[(arene)RuCl_2]_2$ in the presence of sodium methoxide, neutral compounds **1**−**6** have been obtained (Scheme 2), which are soluble in most organic solvents and also in water. Compounds **1** and **3** were then reacted with $AgBF_4$ in acetonitrile, containing small amounts of water, affording the cationic hydrated compounds **7** and **8** (Scheme 2). IR and ^1H and ^{13}C NMR data confirm their proposed structure, in accordance with similar compounds previously reported.[17]

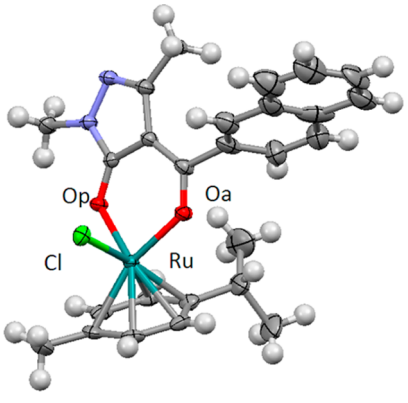

Figure 2. X-ray crystal structure of [Ru(η^6-cymene)(Q^{Napht})Cl] (**3**).

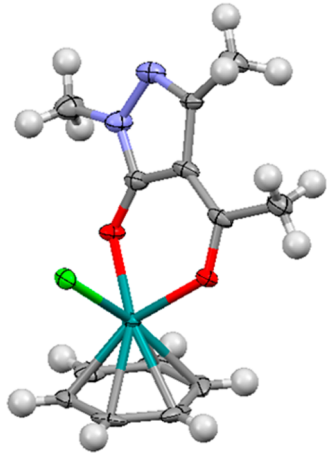

Figure 3. X-ray crystal structure of [Ru(η^6-benzene)(Q^{Me})Cl] (**4**).

Figures 2 and 3 show the molecular structures of compounds **3** and **4**, determined using single-crystal X-ray diffraction, displayed with ellipsoids at 50% probability. When comparing the coordination sphere of both molecules (see Table 2), we see that Ru−Cl distances are equivalent. In contrast, Ru−O(pyrazolonato) {= Ru−Op} and Ru−O(acyl) {= Ru−Oa} differ in [Ru(η^6-*p*-cymene)(Q^{Naph})Cl] (**3**) but are equal in [Ru(η^6-benzene)(Q^{Me})Cl] (**4**). In a Ti-Q antitumor compound,[28] a Ti−Op bond distance shorter than Ti−Oa is observed, which may be associated with a coordinative bond by the acyl group. Both Ru−Cl bond distances are in agreement with the related 40 structures stored in the crystallographic database (CSD) having the framework "RuO_2Cl(arene);" 34 of them are *p*-cymene compounds. The mean Cl−Ru−O bond angle (84.7°) in the CSD compares well with that observed in both structures (85.2° (compound **3**) and 84.3° (compound **4**)). Also the CSD mean values of both the Ru−O (2.091 Å) and the Ru−Cl (2.416 Å) bond distances are coincident with values found for both structures.

The arene−centroid can be considered a fourth bond in a potential tetrahedral arrangement, an alternative to the "piano-stool" description by Sadler[3] where Cl, Op, and Oa are the legs.

dx.doi.org/10.1021/ic403170y | Inorg. Chem. 2014, 53, 3668−3677

Table 2. Geometrical Features in the Coordination Sphere of Compounds 3 and 4; Cen Stays for the Arene Ring Centroid; Op = O(pyrazolonato), Oa = O(acyl)

	Ru−Cl	Ru−Op	Ru−Oa	Ru−Cen	Cen−Ru−Cl	Cen−Ru−Op	Cen−Ru−Oa
3	2.4143(9)	2.079(2)	2.101(2)	1.642	129.6	127.2	126.5
4	2.418(2)	2.095(5)	2.091(4)	1.650	130.4	128.3	125.5

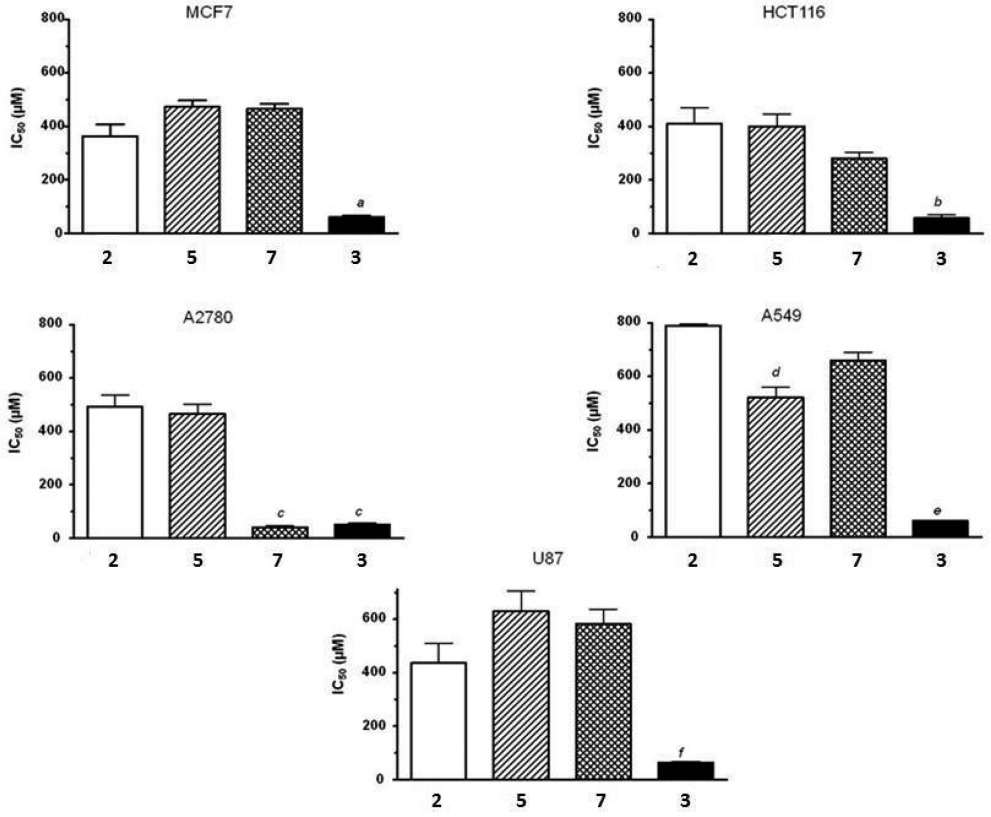

Figure 4. Antiproliferative effect of [Ru(η^6-*p*-cymene)(Q^{Ph})Cl] (**2**), [Ru(η^6-*p*-cymene)(Q^{Naph})Cl] (**3**), [Ru(η^6-hmb)(Q^{Me})Cl] (**5**), and [Ru(η^6-*p*-cymene)(Q^{Me})(H_2O)]BF_4 (**7**) on MCF-7, HCT116, A2780, A549, and U87 human cancer cells. IC_{50} values (μM) are the means ± SE of three or four independent experiments and were extrapolated from dose response curves obtained at the end of 72 h of incubation in the presence of the compounds. a, $p < 0.001$ vs 2, 5, and 7; b, $p < 0.01$ vs 2 and 5, $p < 0.05$ vs 7; c, $p < 0.001$ vs 2 and 5; d, $p < 0.001$ vs 2; e $p < 0.001$ vs 2, 5 and 7; f, $p < 0.05$ vs 2, $p<0.01$ vs 5 and 7.

Table 3. Antiproliferative Effect of Four Ru-arene-Q compounds on MCF-7, HCT116, A2780, A549, and U87 Human Cancer Cells. IC_{50} Values (μM) are the Means ± SE of Three or Four Independent Experiments and Were Extrapolated from Dose Response Curves Obtained at the End of 72 h of Incubation in the Presence of the Compounds

	2	5	7	3
MCF7	363 ± 44	474 ± 23	475 ± 19	61 ± 5[a]
HCT116	409 ± 59	401 ± 45	280 ± 24	57 ± 12[b]
A2780	494 ± 41	465 ± 37	41 ± 5[c]	51 ± 5[c]
A549	790 ± 5	522 ± 38[d]	661 ± 30	60 ± 3[e]
U87	437 ± 73	631 ± 76	614 ± 56	64 ± 5[f]

[a] $p < 0.001$ vs 2, 5, and 7. [b] $p < 0.01$ vs 2 and 5, $p < 0.05$ vs 7. [c] $p < 0.001$ vs 2 and 5. [d] $p < 0.001$ vs 2. [e] $p < 0.001$ vs 2, 5, and 7. [f] $p < 0.05$ vs 2, $p < 0.01$ vs 5 and 7.

This centroid subtends bond angles in the range of 126−129° in compound **3** and 125−128° in compound **4**, that is, making the other 3 "tetrahedral" bond angles (Op−Ru−Cl, Op−Ru−Oa, Oa−Ru−Cl) closer together, probably due to the bulky arene group (see Table 2). In the 40 CSD stored structures, the mean angles of (arene−centroid)−Ru−O and (arene−centroid)−Ru−Cl are identical (129.5°); Table 2 shows equivalence in structures **3** and **4** for (arene−centroid)−Ru−Cl and smaller angles for (arene−centroid)−Ru−O. The (arene−centroid)−Ru distance is 1.642 Å (compound **3**) and 1.650 Å (compound **4**). This may suggest a stronger arene−Ru binding in the former, probably due to the donor features of Me and isopropyl substituents in *p*-cymene. However, the range of this distance in CSD stored structures (1.63 Å−1.66 Å) also includes the value shown by compound **4**. No arene = benzene compounds are included in the 40 stored structures to make a comparison. Interestingly, even if *p*-cymene possesses larger substituents than benzene, it does not affect the coordination sphere geometry (except for the slightly stronger arene−Ru bond). Since this ligand is a natural product it might be preferable for interaction with DNA, especially since the benzene ligand, used in **4**, is carcinogenic.

We were stimulated to explore the antitumor activity of Ru-(4-acylpyrazolon-5-ato) compounds after seeing the pioneering work by Sadler with classical diketones such as acetylacetonato[15] and after studying the antitumor activity of an equivalent

dx.doi.org/10.1021/ic403170y | Inorg. Chem. 2014, 53, 3668−3677

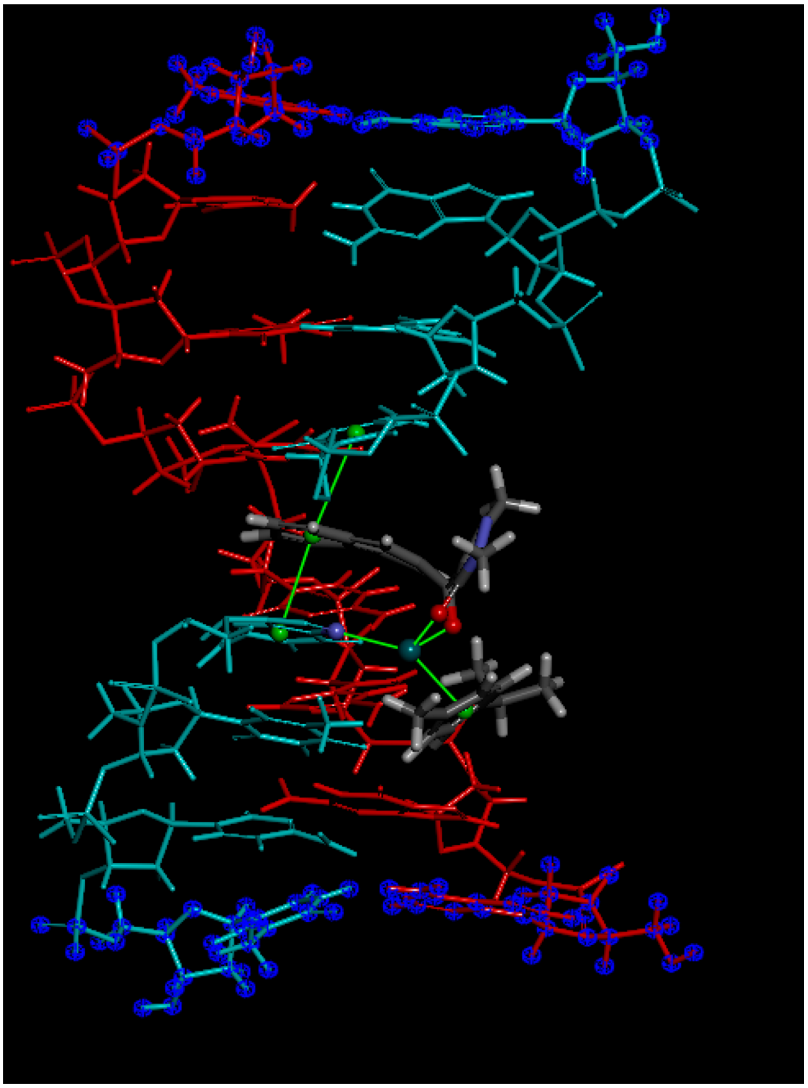

Figure 5. Conformation 952 for the whole DNA−Ru(*p*-cymene)Q^{Naph} system; water and counterions are omitted. In this model the cationic coordination complex is shown as wide stick style, except for coordinated atoms, as ball style; N7(guanine) is purple ball style; bonds in the coordination sphere are solid green. The *p*-cymene moiety is located on the right lower area of the complex, showing a green arene centroid bound to Ru. Both DNA terminal pairs are blue marked, indicating that they were fixed during the dynamic cascade. One DNA helix is red, and the other is aquamarine; $\pi-\pi$ stacking interactions, involving DNA bases with the Q^{Naph} ligand, are depicted as solid green lines.

species containing a natural β-diketone, curcumin, coordinated to a Ru^{II}(*p*-cymene) species.[16] Moreover, recent studies have shown that peripheral variation in the anionic ligand of Ru(arene) compounds can establish interstrand DNA connections,[29] suggesting options for extended interaction far from the metal coordination sphere. Indeed, our idea was to look for some ligand moiety interaction with DNA through intercalation, a widely explored structural feature associated with significant biological activity.[30] In Sadler's work intercalation due to special arenes was linked to increased antitumor activity,[12] but, to our knowledge, the role of the anionic ligands as intercalating agents is much less explored. For instance, antitumor studies in Ru structures having an anionic ligand with a naphthalimide substituent were less efficient than those having an arene-substituted naphthalimide.[31] In addition, although 9-aminoacridine was suggested as a potential ligand for DNA intercalation and coordinated to a Ru(*p*-cymene) framework, its interaction was not described in detail.[32] Furthermore, a review describing the intercalation of Ru(arene) compounds on DNA[3] cited only data based on arenes containing flexible substituents.

We hypothesized that position 4 in 4-acyl-5-pyrazolone ligands was potentially useful for DNA intercalation and performed some preliminary *ab initio* and docking investigations when there was increased aromaticity in position 4. As a result of our findings, we designed this series of Ru-Q-arene complexes. Our experimentally found IC_{50} data (Figure 4 and Table 3) confirm that compound **3**, containing a 4-naphthyl moiety in the ligand Q^{Naph}, has increased antitumor activity for all cell lines, when compared to related 4-methyl and 4-Ph substituted Ru complexes.

Metal affinity for N7(guanine) is widely accepted as a key factor explaining the antitumor activity of cisplatin and Ru(II) complexes.[33,34] Our synthesized model complex [Ru(η^6-*p*-cymene)(Q^{Naph})(9-ethylguanine)]BF_4 (**9**) was easily obtained at room temperature, as shown by ESI-MS data, after simple mixing of [Ru(η^6-*p*-cymene)(Q^{Naph})(H_2O)]BF_4 (**8**) and 9-ethylguanine (Scheme 2), and suggests the feasibility of Ru−N(7) guanine binding. Indeed, the hydrolysis of the related Cl

dx.doi.org/10.1021/ic403170y | *Inorg. Chem.* 2014, 53, 3668−3677

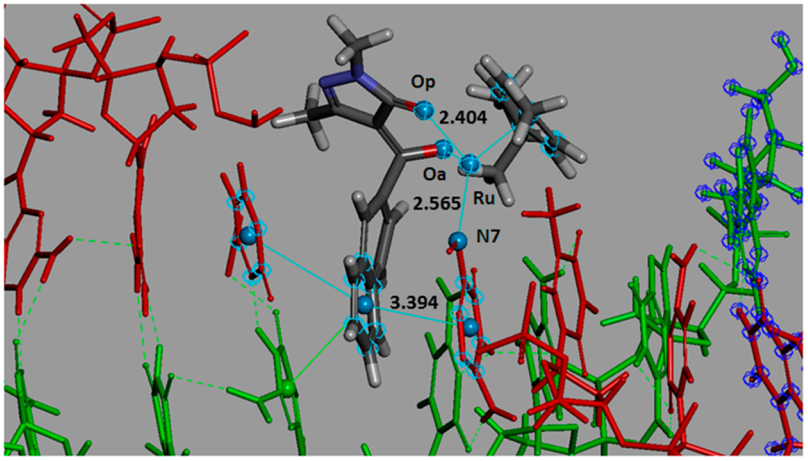

Figure 6. Details of Ru coordination sphere in conformation 952, the minimum energy obtained from the dynamic cascade, showing one helix in red and the other helix in green. The terminal pairs, only one partially shown on the right (blue marked), were fixed during the process. The *p*-cymene ring is on the right area. Light-green dashed lines, indicating H-bonds between DNA bases, are also shown. Some atoms of the red helix are omitted for clarity. Oa = Oacyl and Op = Opyrazolonato correspond to O(carbonyl) and O(hydroxyl), respectively, in Scheme 1.

complex [Ru(η^6-*p*-cymene)(Q^{Naph})Cl] (**3**) to yield the cationic species [Ru(η^6-*p*-cymene)(Q^{Naph})(H_2O)]$^+$ (**8**) is expected to be formed inside the cell, where the chloride concentration is lower. Therefore, a Cl derivative appears to be more protected, as a neutral species, than a cationic complex as shown for cisplatin; for example, it would allow the hydrolyzed "active species" to be generated *in situ*. However, the only biologically tested cationic species in this study (compound **7**), containing a Q^{Me} ligand, is also the most active (A2780 cell line), suggesting that the complex [Ru(η^6-*p*-cymene)(Q^{Naph})(H_2O)]BF_4 (**8**) can be even more active than its parent compound [Ru(η^6-*p*-cymene)(Q^{Naph})Cl] (**3**), as it would combine the naphthyl preference for intercalation, see *infra*, with the cationic feature of **7**. Compound **8** is currently being tested, and results will be published in the near future.

Consequently, compound **3** was selected for a docking study on a DNA octamer, from which conformation 952 has the lowest potential energy and is shown in Figure 5; additional details of the Ru coordination sphere are depicted in Figure 6. The guanine base is linked through N7 to Ru (2.565 Å) and establishes a $\pi-\pi$ interaction with the center of one ring of the naphthyl moiety (3.394 Å); the Ru−Op bond distance is 2.404 Å, and the *p*-cymene ligand protrudes outside the DNA helix. From our docking calculations, we felt that a larger arene such as hexamethylbenzene would hinder the Ru−N7(guanine) binding, although such a restraint would probably not be present if interacting with a single helix.

The arene intercalation may induce strong deformation of the double helix, as observed from NMR data of the 14-base duplex (5′-ATACATGGTACATA-3′)/(3′-TATGTAC-CAT^{17}G^{18}TAT-5′) ruthenated at N7(G^{18}) by [(η6-biphenyl)-Ru(ethylendiamine)]$^{2+}$. One conformer has the biphenyl arene intercalated between G^{18} and T^{17}, while the other has no biphenyl intercalation, but shows T^{17} flipped out of the helix.[35] In contrast, our conformation 952 keeps all the DNA bases in place, as seen in Figure 6 where H-bond interactions between DNA bases are depicted. At present, there is not enough information to determine whether better antitumor activity is induced by more or less helix deformation after ruthenation.

A recent series of ketoamine ligands HL ($HL^{et,Ph}$, $HL^{Ph,Ph}$, and $HL^{Naph,Ph}$), closely related to 4-acyl-5-pyrazones, has been used to synthesize Ru(*p*-cymene)LCl complexes.[36] They have a pendant moiety variant (Et, Ph, and Naph) and so are related to the Met, Ph, and Naph substituents in this study. These Ru complexes were tested against A2780 and A2780R cell lines, but their IC_{50} values did not show a preference for the Ru(*p*-cymene)$L^{Naph,Ph}$Cl, which suggests that the naphthyl moiety does not intercalate with DNA. This appears in contrast with the IC_{50} values for the HL ligands, which show higher activity for $HL^{Naph,Ph}$. It seems, therefore, that ligands containing extended aromatic moieties, such as naphthyl, can intercalate in DNA, but the intercalation mechanism through their Ru(arene) complexes is more subtle.

CONCLUSIONS

Following our theoretical study of Ru(arene)(curcumin)Cl complexes, we designed related potential antitumor compounds Ru(arene)(β-diketonato) using 4-acyl-5-pyrazolone ligands (HQ) to experimentally test ligand intercalation with DNA. Compound Ru(*p*-cymene)Q^{Naph}Cl, containing a peripheral naphthyl moiety in position 4, shows *in vitro* antitumor activity systematically higher than compounds having other substituents in all cell lines. Docking studies show that [Ru(*p*-cymene)(Q^{Naph})Cl] intercalation with DNA is feasible. However, the curcumin ligand activity still is higher than the most active species in the Q series. The present study may stimulate the design of chelating ligands useful for DNA intercalation in metal antitumor compounds

ASSOCIATED CONTENT

Supporting Information

This material is available free of charge via the Internet at http://pubs.acs.org.

AUTHOR INFORMATION

Corresponding Authors

*E-mail: caruso@vassar.edu (F.C.).
*E-mail: fabio.marchetti@unicam.it (F.M.).

Notes

The authors declare no competing financial interest.

■ ACKNOWLEDGMENTS

We thank Jodi Shaulky at Accelrys for helpful discussion. M.R. thanks the HHMI Foundation through Grant 52006322 and the U.S. National Science Foundation, through the Grant 0521237, for the X-ray diffractometer.

■ REFERENCES

(1) Bratsos, I.; Jedner, S.; Gianferrara, T.; Alessio, E. *Chimia* **2007**, *61*, 692−697.
(2) Hartinger, C. G.; Jakupec, M. A; Zorbas-Seifried, S.; Groessl, M.; Egger, A.; Berger, W.; Zorbas, H.; Dyson, P. J.; Keppler, B. K. *Chem. Biodiversity* **2008**, *5*, 2140−2155.
(3) Pizarro, A. M.; Sadler, P. J. *Biochimie* **2009**, *91*, 1198−1211.
(4) Scolaro, C.; Bergamo, A.; Brescacin, L.; Delfino, R.; Cocchietto, M.; Laurenczy, G.; Geldbach, T. J.; Sava, G.; Dyson, P. J. *J. Med. Chem.* **2005**, *48*, 4161−4171.
(5) Martínez, A.; Rajapakse, C. S. K.; Sánchez-Delgado, R. A.; Varela-Ramirez, A.; Lema, C.; Aguilera, R. J. *J. Inorg. Biochem.* **2010**, *104*, 967−977.
(6) Kandioller, W.; Balsano, E.; Meier, S. M.; Jungwirth, U.; Goeschl, S.; ARoller, A.; Jakupec, M. A.; Berger, W.; Keppler, B. K.; Hartinger, C. G. *Chem. Commun.* **2013**, *49*, 3348−3350.
(7) Kurzwernhart, A.; Kandioller, W.; Enyedy, E. A.; Novak, M.; Jakupec, M. A.; Keppler, B. K.; Hartinger, C. G. *Dalton Trans.* **2013**, *42*, 6193−6202.
(8) Aird, R. E.; Cummings, J.; Ritchie, A. A.; Muir, M.; Morris, R. E.; Chen, H.; Sadler, P. J.; Jodrell, D. I. *Br. J. Cancer* **2002**, *86*, 1652−1657.
(9) Wang, F.; Chen, H.; Parsons, S.; Oswald, I. D. H.; Davidson, J. E.; Sadler, P. J. *Chem.—Eur. J.* **2003**, *9*, 5810−5820.
(10) Chen, H.; Parkinson, J. A.; Novakova, O.; Bella, J.; Wang, F.; Dawson, A.; Gould, R.; Parsons, S.; Brabec, V.; Sadler, P. J. *Proc. Natl. Acad. Sci. U.S.A.* **2003**, *100*, 14623−14628.
(11) Morris, R. E.; Aird, R. E.; Murdoch, P. D. S.; Chen, H.; Cummings, J.; Hughes, N. D.; Parsons, S.; Parkin, A.; Boyd, G.; Jodrell, D. I.; Sadler, P. J. *J. Med. Chem.* **2001**, *44*, 3616−3621.
(12) Novakova, O.; Chen, H.; Vrana, O.; Rodger, A.; Sadler, P. J.; Brabec, V. *Biochemistry* **2003**, *42*, 11544−11554.
(13) Chen, H.; Parkinson, J. A.; Morris, R. E.; Sadler, P. J. *J. Am. Chem. Soc.* **2003**, *125*, 173−186.
(14) Liu, H.; Wang, F.; Parkinson, J. A.; Bella, J.; Sadler, P. J. *Chem.—Eur. J.* **2006**, *12*, 6151−6165.
(15) Fernandez, R.; Melchart, M.; Habtemariam, A.; Parsons, S.; Sadler, P. J. *Chem.—Eur. J.* **2004**, *10*, 5173−5179.
(16) Caruso, F.; Rossi, M.; Benson, A.; Opazo, C.; Freedman, D.; Monti, E.; Gariboldi, M. B.; Shaulsky, J.; Marchetti, F.; Pettinari, R.; Pettinari, C. *J. Med. Chem.* **2012**, *55*, 1072−1081.
(17) Marchetti, F.; Pettinari, C.; Pettinari, R.; Cerquetella, A.; Cingolani, A.; Chan, E. J.; Kozawa, K.; Skelton, B. W.; White, A. H.; Wanke, R.; Kuznetsov, M. L.; Martins, L. M. D. R. S.; Pombeiro, A.. J. L. *Inorg. Chem.* **2007**, *46*, 8245−8257.
(18) Caruso, F.; Pettinari, C.; Marchetti, F.; Rossi, M.; Opazo, C.; Kumar, S.; Balwani, S.; Ghosh, B. *Bioorg. Med. Chem.* **2009**, *17*, 6166−6172.
(19) Marchetti, F.; Pettinari, C.; Pettinari, R. *Coord. Chem. Rev.* **2005**, *249*, 2909−2945 and references therein..
(20) Sheldrick, G. M. *Acta Crystallogr.* **2008**, *A64*, 112−122.
(21) *Dmol3 Software;* Accelrys, Inc.; San Diego, CA.
(22) Delley, B. *J. Chem. Phys.* **2000**, *113*, 7756−7764.
(23) Delley, B. *J. Chem. Phys.* **1990**, *92*, 508−517.
(24) Perdew, J. P.; Burke, K.; Ernzerhof, M. *Phys. Rev. Lett.* **1996**, *77*, 3865−3868.
(25) Scudiero, D. A.; Shoemaker, R. H.; Paull, D.; Monks, A.; Tierney, S.; Nofziger, T. H.; Currens, M. J.; Seniff, D.; Boyd, M. R. *Cancer Res.* **1988**, *48*, 4827−4833.
(26) Wu, G.; Robertson, D. H.; Brooks, C. L.; Vieth, M. *J. Comput. Chem.* **2003**, *24*, 1549−1562.
(27) Searle, M. S.; Maynard, A. J.; Williams, H. E. L. *Org. Biomol. Chem.* **2003**, *1*, 60−66.
(28) Caruso, F.; Rossi, M.; Tanski, J.; Sartori, R.; Sariego, R.; Moya, S.; Diez, S.; Navarrete, E.; Cingolani, A.; Marchetti, F.; Pettinari, C. *J. Med. Chem.* **2000**, *43*, 3665−3670.
(29) Brabec, V.; Novakova, O. *Drug. Resist. Updates* **2006**, *9*, 111−122.
(30) Lown, J. W. *Pharmacol. Ther.* **1993**, *60*, 185−214.
(31) Kilpin, K. J.; Clavel, C. M.; Edafe, F.; Dyson, P. J. *Organometallics* **2012**, *31*, 7031−7039.
(32) Ruiz, J.; Vicente, C.; de Haro, C.; Bautista, D. *Dalton. Trans.* **2009**, *26*, 5071−5073.
(33) Dorcier, A.; Hartinger, C. G.; Scopelliti, R.; Fish, R. H; Keppler, B. K.; Dyson, P. J. *J. Inorg. Biochem.* **2008**, *102*, 1066−1076.
(34) Chen, H.; Parkinson, J. A.; Parsons, S.; Coxall, R. A.; Gould, R. O.; Sadler, P. J. *J. Am. Chem. Soc.* **2002**, *124*, 3064−3082.
(35) Liu, H. K.; Berners-Price, S. J.; Wang, F.; Parkinson, J. A.; Xu, J.; Bella, J.; Sadler, P. J. *Angew. Chem., Int. Ed. Engl.* **2006**, *45*, 8153−8156.
(36) Pettinari, R.; Pettinari, C.; Marchetti, F.; Clavel, C. M.; Scopelliti, R.; Dyson, P. J. *Organometallics* **2013**, *32*, 309−316.